

# Atomistic modeling of B activation and deactivation for ultra-shallow junction formation

Maria Aboy\*, Lourdes Pelaz, Luis A. Marqués and Juan Barbolla.

University of Valladolid  
Campus Miguel Delibes, University of Valladolid, 47011  
Valladolid, Spain

\* email: marabo@tel.uva.es

Ali Mokhberi, Yayoi Takamura, Peter B. Griffin and James D. Plummer.

Stanford University  
Stanford, CA, USA

**Abstract**—We have investigated the physical mechanisms for the B clustering formation and dissolution for ultra-shallow junction formation. We have analyzed high-dose low-energy B implants and theoretical structures with box-shaped B profiles that are fully active. These structures could be simplifications of the situation resulting from regrowth of preamorphized or laser annealed B implants. For these conditions, we have to take into account new effects due to the high B concentration and the proximity to the surface. The simulations show that the deactivation mechanism for B implants in crystalline Si takes place through a high interstitial content path, and it happens even for low B doses. The deactivation of the B box depends on the B concentration. In the absence of excess Si interstitials, B deactivation only happens for very high B concentrations. This process is very slow for low temperature anneals. If there is a residual concentration of Si interstitials along with the B box, the deactivation will take place rapidly even at low temperatures. In the model, the reactivation mechanism takes place in all cases through the low interstitial content path, by the capture of native Si interstitial defects and the emission of B interstitials.

*Modeling, Electrical activation, Boron clusters, High concentration.*

## I. INTRODUCTION

Boron ion implantation is the most common process used for establishing p-type dopant profiles in silicon. However, the implanted ions generate a large concentration of defects that deteriorate the device performance[1,2], and the implanted dopant is generally electrically inactive[3,4]. Post-implant thermal annealing is required to anneal out the damage and to electrically activate the dopant. The interaction between boron and silicon interstitials caused by ion implant damage complicates the formation of ultrashallow, low resistivity junctions. During the regrowth of pre-amorphized and laser annealed implants the activation level of the samples is improved[5-7]. It is generally assumed that, during the solid-phase epitaxial (SPE) regrowth of an amorphous layer, boron is incorporated into substitutional positions and thus, becomes electrically active. However, as devices are scaled down, higher carrier concentration levels are needed for ultra-shallow junction formation. In the presence of high B concentrations the complete activation of B in amorphous layers is difficult[6,7]. The activation achieved during

regrowth is very unstable and subsequent thermal treatment results in boron deactivation above a threshold concentration ( $\sim 1-3 \times 10^{20} \text{ cm}^{-3}$ ) [6-9]. Laser annealing makes initial electrical activation up to levels  $\sim 10^{21} \text{ cm}^{-3}$  possible [8]. However, deactivation occurs during additional thermal treatments [10].

Previous work [11-13] concluded that for medium B implant doses in crystalline Si, a pathway with a high interstitial content was driving the B cluster formation responsible for electrical deactivation. B atoms in concentrations in the order of  $10^{19} \text{ cm}^{-3}$  in delta doped marker layers (initially substitutional) formed clusters only when a high Si interstitial concentration was overlapping the B profile. In this work, we analyze the new scenario that arises for very high B concentrations, as those needed for the formation of ultra-shallow junctions. We study the case of a simultaneous presence of high Si interstitial concentration (as corresponds to high dose B implants in crystalline Si) and also when the Si interstitial concentration is low and separated from the B profile (as corresponds to the end of range damage in regrown amorphous layers). For the later case, we consider theoretical box-shaped B profiles initially fully active in the presence of different Si interstitial profiles or with only equilibrium Si interstitials.

## II. PHYSICAL MODELING

To analyze the deactivation and reactivation mechanisms for high B concentration profiles we carried out atomistic simulations based on kinetic Monte Carlo modeling of dopant diffusion and defect interactions in Si. We use a binary collision approximation code, MARLOWE[14], to generate coordinates of the displaced atoms in the lattice along with those of the implanted atom. These coordinates are transferred to the non-lattice kinetic Monte Carlo diffusion code DADOS[15]. Defects experience diffusion or emission events according with their respective rates at each temperature. Dynamic annealing during the implant and the ramp up in temperature until reaching the target temperature is included in the model. Defects interact with each other when they are within a second neighbour distance of each other. The B clustering model includes a complex pathway for B/Si interstitial interactions leading to  $B_n I_m$  complexes responsible for B deactivation[11-13] (Fig. 1). The predominance of a

given pathway is determined by the clusters energies and by the B and Si interstitial concentrations. In the boron clustering model proposed by Pelaz et al. [11-13] there are two different main pathways for the formation of the boron clusters. In the low interstitial content path, the B cluster formation is through the capture of mobile  $B_i$  by the preexisting clusters and the rapid release of Si interstitials, leaving B clusters with low interstitial content. In the high interstitial content path, Si interstitials are not emitted rapidly, resulting in B clusters rich in Si interstitials. Those interstitials are released later on during the anneal when the Si interstitial supersaturation decreases.

### III. FORMATION AND DISSOLUTION OF BORON-INTERSTITIAL CLUSTERS (BIC's)

We have analyzed the activation mechanism in high-dose ultra-low energy B implants and high temperature annealing, as is the case of a 1 keV  $1 \times 10^{15} \text{ cm}^{-2}$  B implant into crystalline Si, annealed at different temperatures ranging from 910 to 1010 °C. In Fig. 2 we compare the active fraction experimentally obtained from Hall measurements [16], with the substitutional B resulting from our simulations. Simulation results are in very good agreement with the experimental data, which gives validity to the model. The B cluster formation and growth starts during the implant and continues during temperature ramp-up, as can be seen in Fig. 3 and Fig. 4. There is a large fraction of interstitials in the B complexes indicating that B clusters are formed through the high interstitial content path ( $B_n I_m + Bi \rightarrow B_{n+1} I_{m+1}$ ), similar to the results observed for lower dose implants [11-13]. By the time the target temperature is reached the maximum deactivation has already occurred. The resulting clusters (mostly  $B_4 I_m$ ) emit Bi and Si interstitials (resulting  $B_3 I_{m-1}$  or  $B_4 I_{m-1}$ ) and end up in B clusters with a low interstitial content ( $B_4, B_3, B_2$ ) that only can dissolve by the capture of an equilibrium Si interstitial and the emission of Bi ( $B_2 + I \rightarrow B_2 I \rightarrow B + Bi$ ) (Fig 4).

The situation is quite different when B is implanted in preamorphized Si. For low B concentrations, B atoms are incorporated into the lattice at the same time that the excess atoms existing in the amorphous layer are swept towards the

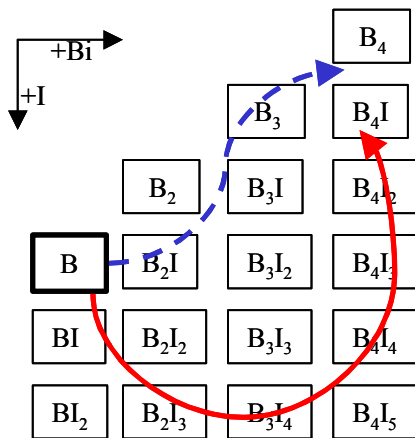


Fig. 1. Schematic of the boron-interstitial clusters ( $B_n I_m$ ) pathways. The solid line represents the high interstitial content path. The dashed line represents the low interstitial content path.

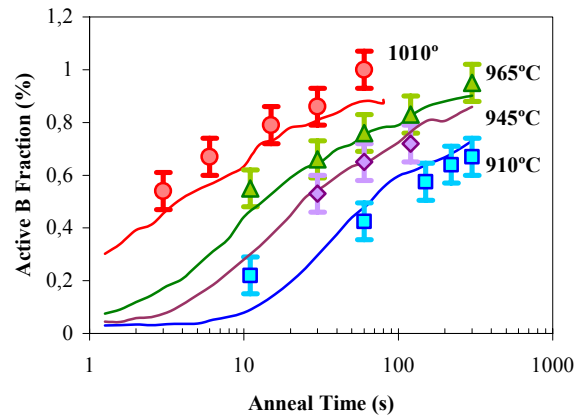


Fig. 2. Time evolution during annealing of the active B fraction for a 1 keV  $10^{15} \text{ cm}^{-2}$  B implant. Symbols correspond to experimental values obtained from Hall measurements. Lines correspond to simulated substitutional B.

surface during the regrowth. Therefore, after regrowth B is electrically active and no excess interstitials overlap with the B profile. The small Si interstitial supersaturation set by the end of range defects at the original amorphous/crystalline interface is not enough to deactivate the B during additional anneals. Nevertheless, it has been observed that in the presence of high B concentrations the activation during annealing is not complete. Because of the uncertainties in the status resulting after the regrown process we have carried out simplified simulations that can approximate the real case. Those consist of box like shaped B substitutional (electrically active) profiles 10 nm thick with concentrations ranging from  $10^{20}$  to  $10^{21} \text{ cm}^{-3}$  (approximately corresponding to a low energy B implant to a dose of  $10^{15} \text{ cm}^{-2}$ ). In the absence of any excess Si interstitials, the deactivation of B will only happen if the B concentration is high enough (Fig. 5). Since only the equilibrium interstitial concentration is present, the B

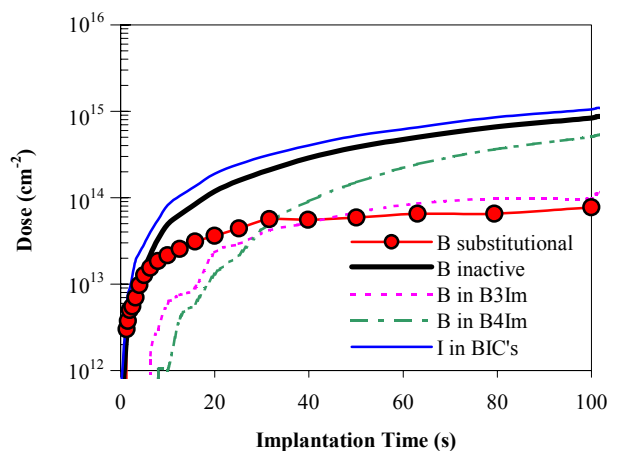
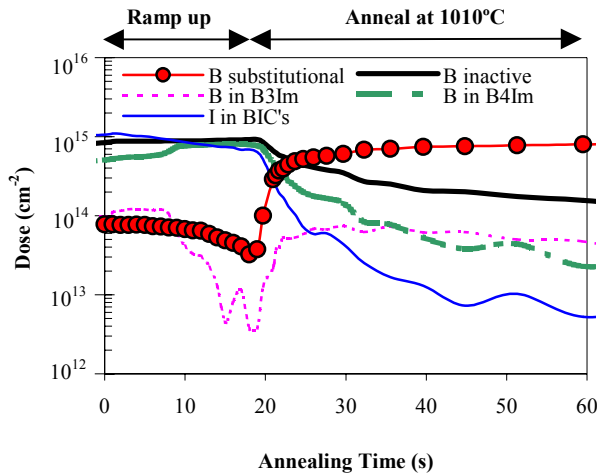


Fig. 3. Evolution of the B complexes during the 1 keV  $10^{15} \text{ cm}^{-2}$  B implant. The total B dose is increasing as the implantation proceeds. By the end of the implantation most of the B introduced is in complexes ( $B_n I_m$ ). The number of interstitials in B complexes (I in BIC's) is even higher than the number B atoms, indicating the formation of complexes of high interstitial content.



**Fig. 4.** Evolution of the B complexes during the annealing at 1010°C. The dissolution of the  $B_4I_m$  complexes leads to smaller B complexes and with less interstitial content.

deactivation can only take place through the low interstitial content path, by capturing Bi and emitting some Si interstitials ( $B_nI_m + Bi \rightarrow B_{n+1}I_{m+1} \rightarrow B_{n+1}I_m + I$ ). This is shown in Fig. 6 by the fact that there is a small fraction of Si interstitials in the B clusters during the formation stage. The reactivation also takes place through the low interstitial content path through the reverse reactions of the formation. The deactivation mechanism is extremely slow at low temperatures but it happens rapidly at high temperatures (Fig. 7). Similar behavior is observed experimentally during thermal anneals of samples previously laser annealed [10].

The presence of an excess of Si interstitials along with the B box could represent the end of range damage resulting from preamorphizing implants or the damaged region that has not been melted during laser treatment or residual defects from an imperfect regrowth. The active B fraction during the annealing

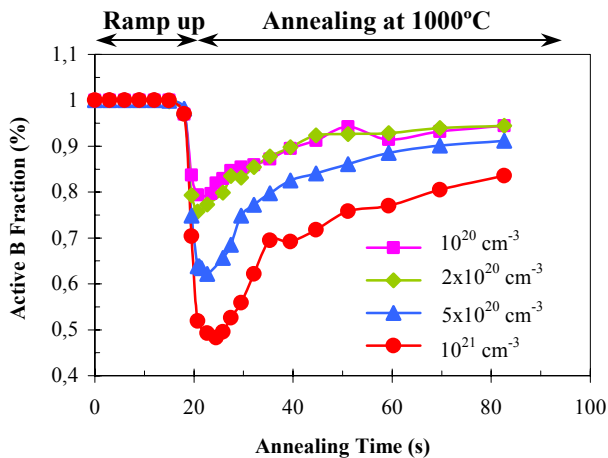


**Fig. 5.** Active B fraction of B boxes of 10 nm wide and different concentrations corresponding to doses going from  $10^{14} \text{ cm}^{-2}$  to  $10^{15} \text{ cm}^{-2}$ . There are no excess interstitials. For the lower B concentration the deactivation is small. Additional annealing time improves the activation of high B concentration profiles.

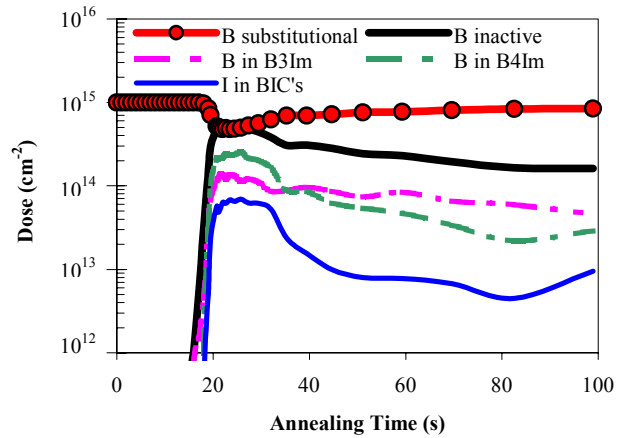


**Fig. 6.** Evolution of the B complexes during annealing at 1000°C of a box shaped B profile 10 nm wide and concentration of  $10^{21} \text{ cm}^{-3}$ . The number of interstitials in the B complexes is significantly lower than the number of B atoms, indicating that the formation of those complexes follows the low interstitial content path.

at  $\sim 1000^\circ\text{C}$  is compared for B implants and box-shaped B profiles with and without excess Si interstitials for a B dose of  $10^{14} \text{ cm}^{-2}$  (Fig. 8) and  $10^{15} \text{ cm}^{-2}$  (Fig. 9). The simulations show that at low B concentrations ( $< 10^{20} \text{ cm}^{-3}$ ), the initially fully active B hardly forms B clusters unless the Si interstitial profile overlaps with the B profile. When this happens (for example, a B implant in crystalline Si), B deactivates for concentrations significantly lower than the B solubility. However, the injection of Si interstitials from a Si interstitial defect band existing deeper into the bulk is not enough to deactivate B. This result is consistent with the experimental observation that for low B concentration, B activates during regrowth and does not deactivate with an additional anneal. On the contrary, for high B concentrations ( $> 1\text{-}3 \times 10^{20} \text{ cm}^{-3}$ ), the presence of only equilibrium Si interstitials is enough to partially deactivate the B atoms. The presence of excess interstitials accelerates the process.

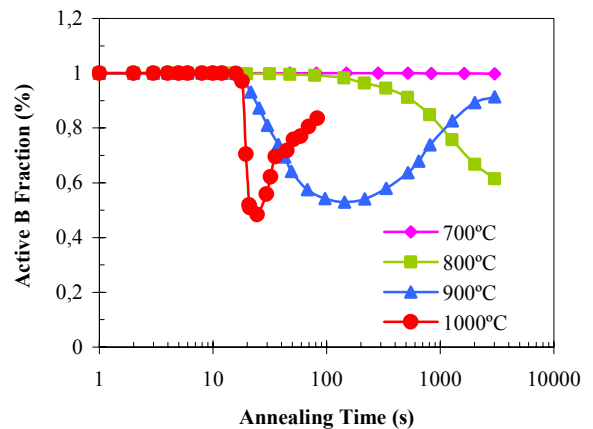


**Fig. 7.** Active B fraction as a function of the annealing time for different annealing temperatures of a box shaped B profile of 10 nm wide and concentration of  $10^{21} \text{ cm}^{-3}$ . The deactivation occurs with the equilibrium interstitial concentration. At low temperatures the process is very slow.

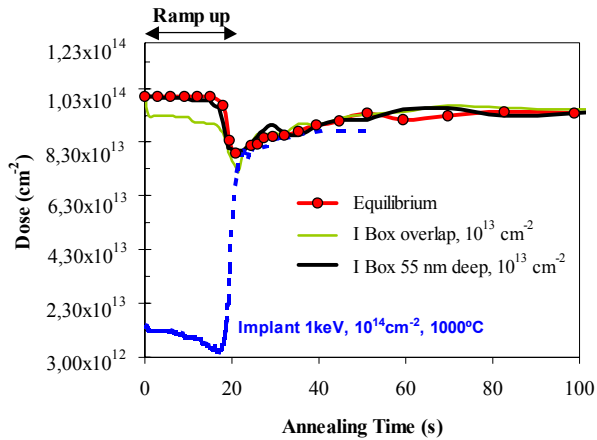


**Fig. 8.** Active B fraction of a box shaped B profile 10 nm wide and concentration of  $10^{20} \text{ cm}^{-3}$  annealed at  $1000^\circ\text{C}$  in the presence of different Si interstitial profiles. The case corresponding to a B implant of  $10^{14} \text{ cm}^{-2}$  is also included for comparison. The deactivation is small in the absence of excess Si interstitial and it is significant in the implant case.

#### IV. CONCLUSIONS

We investigated the physical mechanisms for the B clustering formation and dissolution for ultra-shallow junction formation. We analyzed high-dose low-energy B implants and theoretical structures with fully active, box-shaped B profiles. These structures could be simplifications of the situation resulting after regrowth of preamorphized or laser annealed B implants. We showed that the deactivation mechanism for B implants in crystalline Si takes place through a high interstitial content path, and it happens even for low B doses. For the box-shaped B profiles, the deactivation depends on the B concentration. In the absence of excess Si interstitials, B deactivation only happens for very high B concentrations. If there is a residual concentration of Si interstitials along with the B box, the deactivation will take place rapidly even at low temperatures. The reactivation mechanism takes place in all cases through a low interstitial content path, by the capture of native Si interstitial defects and the emission of B interstitials.

#### REFERENCES

- [1] D. J. Eaglesham, P. A. Stolk, H.-J. Gossmann, and J. M. Poate, *Appl. Phys. Lett.* 65, 2305 (1994).
- [2] P. A. Stolk, D. J. Eaglesham, H.-J. Gossmann, and J. M. Poate, *Appl. Phys. Lett.* 66, 1370 (1995).

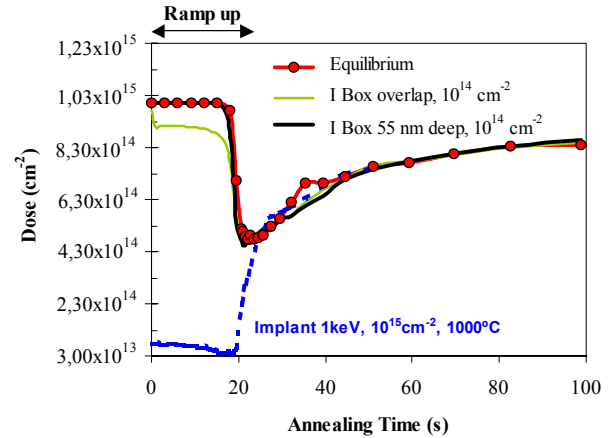


**Fig. 9.** Active B fraction of a box shaped B profile 10 nm wide and concentration of  $10^{21} \text{ cm}^{-3}$  annealed at  $1000^\circ\text{C}$  in the presence of different Si interstitial profiles. The case corresponding to a B implant of  $10^{15} \text{ cm}^{-2}$  is also included for comparison. The deactivation is significant even with the equilibrium Si interstitial concentration.

- [3] N. E. B. Cowern, K. T. F. Janssen, and H. F. F. Jos, *J. Appl. Phys.* 68, 6191 (1990).
- [4] P. A. Stolk, H.-J. Gossmann, D. J. Eaglesham, D. C. Jacobson, and J. M. Poate, *Appl. Phys. Lett.* 66, 568 (1995).
- [5] M. Y. Tsai and B. G. Streetman, *J. Appl. Phys.* 50, 183 (1979).
- [6] E. Landi, A. Armigliato, S. Solmi, R. Kögler, and E. Wieser, *Appl. Phys. A* 47, 359 (1998).
- [7] A. Mokhberi, L. Pelaz, M. Aboy, L. Marques, J. Barbolla, P. Griffin, J. D. Plummer, E. Paton, S. McCoy, J. Ross, K. Elliot and J. Gelpi, *IEDM Proceedings* 2002.
- [8] S. Solmi, E. Landi, and F. Baruffaldi, *J. Appl. Phys.* 68, 3250 (1990).
- [9] V. Privitera, E. Napolitani, F. Priolo, S. Moffatt, A. La Magna, G. Mannino, A. Carnera, A. Picariello, *Materials Sci. Semiconductor Proc.* 2, 35 (1999).
- [10] Y. Takamura, S. H. Jain, P.B. Griffin, and J.D. Plummer, *J. Appl. Phys.* 92, 230 (2002).
- [11] L. Pelaz, M. Jaraiz, G. H. Gilmer, H.-J. Gossmann, C. S. Rafferty, D. J. Eaglesham, and J. M. Poate, *Appl. Phys. Lett.* 70, 2285 (1997).
- [12] L. Pelaz, G. H. Gilmer, H.-J. Gossmann, J. M. Poate, C. S. Rafferty, M. Jaraiz, and J. Barbolla, *Appl. Phys. Lett.* 74, 3657 (1999).
- [13] L. Pelaz, V. C. Venezia, H.-J. Gossmann, G. H. Gilmer, A. T. Fiory, C. S. Rafferty, M. Jaraiz, and J. Barbolla, *Appl. Phys. Lett.* 75, 662 (1999).
- [14] M. T. Robinson and I. M. Torrens, *Phys. Rev. B* 9, 5008 (1974).
- [15] M. Jaraiz, L. Pelaz, J. E. Rubio, J. Barbolla, G. H. Gilmer, D. J. Eaglesham, H.-J. Gossmann, and J. M. Poate, *Mater. Res. Soc. Symp. Proc.* 532, 43 (1998).
- [16] Ali Mokhberi, Peter B. Griffin, James D. Plummer, Eric Paton, Steve McCoy, and Kieffer Elliott, *IEEE Trans. Electron Devices* 49, 1183 (2002).